# Landsat-7 ETM+: 12 years On-Orbit Reflective-Band Radiometric Performance

Brian L. Markham, *Member, IEEE,* Md. Obaidul Haque, Julia A. Barsi, Esad Micijevic,

Dennis L. Helder*, Senior Member, IEEE,* Kurtis J. Thome, David Aaron and Jeffrey S.

Czapla-Myers

*Abstract*— The Landsat-7 ETM+ sensor has been operating on orbit for more than 12 years and characterizations of its performance have been ongoing over this period. In general, the radiometric performance of the instrument has been remarkably stable: (1) Noise performance has degraded by 2% or less overall, with a few detectors displaying step changes in noise of 2% or less, (2) Coherent noise frequencies and magnitudes have generally been stable, though the within-scan amplitude variation of the 20kHz noise in bands 1 and 8 disappeared with the failure of the scan line corrector and a new similar frequency noise (now about 18kHz) has appeared in two detectors in band 5 and increased in magnitude with time, (3) Bias stability has been better than 0.25 DN out of a normal value of 15 DN in high gain, (4) Relative gains, the differences in response between the detectors in the band, have generally changed by 0.1% or less over the mission, with the exception of a few detectors with a step response change of 1% or less and (5) Gain stability averaged across all detectors in a band, which is related to the stability of the absolute calibration, has been more stable than the techniques used to measure it. Due to the inability to confirm changes in the gain (beyond a few detectors that have been corrected back to the band average),

B. L. Markham is with the NASA Goddard Space Flight Center (GSFC), Greenbelt, MD 20771 USA (phone: 301-614-6608; fax: 301-614-6695; e-mail: Brian.L.Markham@nasa.gov).
Md. O. Haque is with SGT, Inc., contractor to the USGS Earth Resources Observation and Science (EROS) Center, Sioux Falls, SD, 57198 USA (e-mail: ohaque@usgs.gov).
J. A. Barsi is with SSAI, Inc, GSFC, Greenbelt, MD 20771 USA (email: Julia.A.Barsi@nasa.gov).
E. Micijevic is with SGT, Inc., contractor to the USGS Earth Resources Observation and Science (EROS) Center, Sioux Falls, SD, 57198 USA (e-mail: emicijevic@usgs.gov).
D. H. Helder is with the College of Engineering, South Dakota State University, Brookings, SD 57007 USA (e-mail: Dennis.Helder@SDSTATE.edu).
K. J. Thome is with the NASA Goddard Space Flight Center (GSFC), Greenbelt, MD 20771 USA (e-mail: Kurtis.Thome@nasa.gov).
D. Aaron is with the Department of Physics, South Dakota State University, Brookings, SD 57007 USA (e-mail: David.Aaron@SDSTATE.edu).
J. Czapla-Myers is with the College of Optical Sciences, University of Arizona, Tucson, AZ 85721-0094 USA (e-mail: j.czapla-myers@optics.arizona.edu).

ETM+ reflective band data continues to be calibrated with the pre-launch measured gains. In the worst case some bands may have changed as much as 2% in uncompensated absolute calibration over the 12 years.

*Index Terms*—Landsat, radiometry, ETM+, calibration

## I.  INTRODUCTION

Landsat-7 has been on-orbit and collecting Earth imagery with its Enhanced Thematic Mapper Plus (ETM+) sensor since April 1999.  The ETM+ is a derivative of the Thematic Mapper (TM) sensors flown on Landsats 4 and 5.  Salient characteristics of the ETM+ are presented in table 1.  The ETM+ has been well described in a number of publications, e.g., the Landsat Science Data Users Handbook [1], as have its on-board radiometric calibration capabilities, pre-launch radiometric characterization [2], and early on-orbit radiometric characterization and calibration [3,4]. Among the radiometric characteristics evaluated during the first few years on orbit were noise, both overall and coherent; stability, both in terms of biases and gain; and artifacts, for example, detector ringing.

The radiometric stability of the instrument for the first 4 years on orbit was generally better than the techniques used to detect any changes [4,5].  An independent study [6] also could not find trends in the ETM+ response through 2003 to within the uncertainty of their methods.  A more recent study covering the time period through 2008, using some of the same Pseudo Invariant Calibration Sites (PICS) as used in [3], continued to show no definitive trend in the ETM+ response [7]. The relative gains (detector-to-detector within a band), with the exception of a few detectors that had small jumps or dips in response at up to the 2% level, changed less than 0.1%  over the period.

The objective of this study was to extend the radiometric assessment of ETM+ and its on-board calibrators over the current lifetime of the mission.  In particular, the analyses conducted in [3] and [4] were extended.

The Image Assessment System (IAS), a portion of the Landsat-7 ground system, has the responsibility for monitoring the performance of the ETM+ instrument and the quality of the data products. The IAS is

staffed by USGS calibration analysts in conjunction with the NASA Land-cover satellite Project Science Office (LPSO) analysts. Results are reported regularly at internal Landsat Calibration Working Group (LCWG) meetings. The LCWG consists of the IAS teams from USGS and NASA and outside investigators typically involved in vicarious calibration of the ETM+ reflective and thermal bands. Members of this group conducted the analyses in this paper.

## II. ETM+ Noise characterization

### A. *Total Noise*

The analysis discussed in [3] was extended over the current mission lifetime. Basically, solar diffuser images collected across a range of solar illumination angles during monthly 15 minute collects, provided the data sets for measuring the noise as a function of radiance. An equation of the form:

$$NE\Delta L = (a+b*L_\lambda)^{0.5}$$

was fit to the data, where NE$\Delta$L is noise equivalent change in radiance (W/m$^2$ sr µm), $L_\lambda$ is the radiance, and a ((W/m$^2$ sr µm)$^2$) and b (in W/m$^2$ sr µm) are fitting parameters. From this equation the noise is evaluated at two radiance levels, "typical" and "high". In figure 1 are shown the trends for the typical and high radiance levels for band 3, after converting noise to signal-to-noise ratio (SNR).

Several observations from figure 1: (1) the overall change in noise over almost 12 years of data collection is small, i.e., less than 2% for most detectors, (2) the low radiance SNR trend is noisy between years 2 and 4, (this is an artifact due to short acquisitions being taken at this time, so that noise performance at the typical radiance level was extrapolated) and (3) one detector (#6) experienced a step-like change in noise of about 2% in year 9. These patterns, consisting of trends on the order of 1% with occasional channels that have a small step-like decrease in SNR, are typical for all bands. Table 2 presents those detectors that have exhibited step changes in noise response. Overall the instrument has been maintaining its noise performance well.

*B. Coherent Noise*

Coherent or pattern noise is a component of the total noise discussed above. As described in [3], Fast Fourier Transforms (FFT's) on night (dark) scenes are used to characterize coherent noise. Four types of coherent noise have previously been observed on ETM+ [2]. Figure 2 shows the power history for the coherent noise types using representative detectors for each noise type.

The panchromatic band (band 8) 104 kHz noise (half cycle per pixel) is one of the most consistent and is the highest power (~ 0.13 $DN^2$ in low gain mode) found in ETM+ data with the exception of the inconsistent noise in band 5 detectors #12 and #10. A subtractive correction algorithm is implemented to eliminate this panchromatic band noise in the Landsat Level 1 Product Generation System at USGS EROS. Figure 2 shows the lifetime trend of 104 kHz coherent noise of band 8 detector #3.

The 4.9 kHz (one cycle per ~20 pixels) coherent noise is found in the primary focal plane bands. Bands 2, 3 and 8 are most affected. The power of this noise is usually less than 0.05 $DN^2$ and varies from detector to detector. For a specific detector it is very stable over the mission lifetime except at the time of the scan line corrector (SLC) failure (May 2003) when a slight decrease of this noise power was detected in some detectors. Figure 2 depicts the nature of this noise power for three representative detectors from bands 2, 3 and 8.

The 20 kHz noise has changed over the mission lifetime. Band 8 detector #5 noise encountered a sharp increasing trend for few months prior to the scan line corrector failure and then decreased and maintained stability, except for a few fluctuations, for the rest of the life. Band 1 detector #9 noise also increased slightly before the SLC failure. The 20 kHz noise of this detector decreased with SLC failure to such a level that it is almost undetectable by IAS. Figure 2 shows lifetime trends of band 8 detector #5 and band 1 detector #9 coherent noise power as estimated using IAS trended database.

The anomalous nature of the 20kHz noise [3], where the noise power decreases from the shutter region towards the center of a scan line, disappeared with SLC failure. The occasional ringing events [3] continue, characterized by large amplitude 20kHz oscillations that exponentially decrease in amplitude with time.

Band 1 detectors #9 and #14 and band 8 detector #1 are most affected by 20 kHz noise powered by ringing events.

The band 5 detector #10 and #12 coherent noise, identified as 20kHz noise for the first few years after launch [3], has changed both in power and frequency. This noise behavior is considerably different from that of the other detectors affected by 20 kHz noise and will be considered a fifth type of coherent noise. At present the peak frequency of this noise is around 18 kHz. Although the noise peak frequency shows a decrease over mission lifetime, the noise power has increased significantly (Figure 2). This noise was almost undetectable until 2007 and then started to increase gradually followed by rapid increase after switching to bumper mode operation in April 2007. This noise frequency and power are highly correlated to instrument time-on. Figure 3 shows the decaying trend of band 5 detector #12 noise power with instrument time-on as seen from February 29, 2010 night data collected at the beginning of FASC acquisition. Due to this decaying effect, only a few ETM+ scenes at the beginning of an interval are visibly affected by this coherent noise.

The 5.6 kHz noise of band 3 detector #4 with varying power was occasionally present in ETM+ data before mid 2005. Since mid 2005, this low power noise occurs more regularly. The noise power is around $0.02 \text{ DN}^2$ as found from band 3 night data collected in low gain mode.

Overall the coherent noise behavior of the ETM+ has changed relatively little over the mission lifetime with some improvement in the band 1 and 8 20kHz noise, particularly near the edges of the images after the scan line corrector failure and an increase in the band 5 20 kHz (now 18kHz) noise in two detectors. The band 5 noise is only visually objectionable for the first few scenes after instrument turn-on and decreases to levels that should be acceptable for most users after this time.

III.  ETM+ Radiometric stability

### A.  Detector Bias Stability

Each detector's bias, or output for zero signal input, is measured at the end of each scan line when the shutter passes in front of the focal plane.  Nominally 10 DN for low gain and 15 DN for high gain, the levels vary slightly among detectors. Band 5 detector #9 shows the largest long-term change in bias, though it is only about 0.25 DN (Figure 4). Band 5 detector #4, shown in [3] as an example for detectors with very stable biases, has continued to be stable (Figure 5).  Note that the bias is corrected line-by-line in Landsat product generation and the amount of change in bias is small enough to have no significant impact on the dynamic range of the system, so these changes have essentially no impact on the usability of the ETM+ data.  That the bias levels are very stable over time is a general indication of the stability and health of the electronics of the system.

### B.  Relative Gain Stability (detector-to-detector)

The ETM+ has multiple detectors per band (table 1). Each detector has a similar responsivity or gain, generally varying by no more than ± 1% within a band. The relative gains, here defined as the ratios of each detector's gain to the band-average gain, are measured on-orbit by using the bright uniform images provided by the sun illuminated diffuser as well as Earth image statistics. The relative gain is determined by ratioing a particular detector's net response (having subtracted the bias) to the band-average net response. When a relative gain changes by about 0.2% or more for at least two consecutive diffuser acquisitions (generally about 2 months), the calibration parameter file is updated so as to limit striping in processed ETM+ data.

The relative gains of the ETM+ bands have continued to be extremely stable, with an occasional detector changing up to 1% in a step-like fashion.  Band 1 (Figure 6) has shown no detectors even reaching 0.1% change in relative gain over 12 years on-orbit.  Band 5 (Figure 7) detectors have been somewhat less stable,

but only one detector (#9) has reached the 0.2% threshold with a long-term drift and one dip and recovery of about 0.2%.

### C. Absolute Gain Stability (band average)

A number of techniques are used to monitor the stability of the absolute radiometric calibration of the ETM+ bands.  These include on-board calibrator and vicarious calibration methods.

The ETM+ has three on-board radiometric calibration systems [2]:  the lamp-based internal calibrator, the direct solar view partial aperture solar calibrator and the diffuser-based full aperture solar calibrator. Previously [4,8], the partial aperture solar calibrator and primary lamp on the internal calibrator have been shown to be unstable over the long term, i.e., changes in output by greater than 1% per year in most bands, whereas the instrument's inherent stability appears to be at least a factor of 5 better than this [4].  Even for the best behaved of the on-board calibrators, the infrequently used lamp 2 of the internal calibrator and the diffuser, the ETM+ variation in response to these devices appears to be more a function of their instability than the ETM+ itself.

The vicarious techniques include calibrations using (1) ground targets independently characterized simultaneously with their acquisition by ETM+, and (2) ground targets that are believed to be inherently stable, i.e., PICS [4].

### 1) On-board calibration results

As indicated, two on-board devices, the internal calibrator with its lamp 2 and the diffuser continue to give useful information on the long-term stability of the ETM+ instrument.  Lamp 1 has been used on the vast majority of the ETM+ acquisitions, whereas lamp 2 was used during the initial on-orbit check out period, about once every two months beginning 3 years after launch and about twice a month beginning 7 years after launch. The FASC diffuser is deployed approximately monthly and the light reflected off the diffuser is used as a calibration signal for the ETM+ [4]. Responses of the ETM+ bands 3, 4, 5 and 7 to lamp #2 and FASC (as well as the other calibration sources and techniques) are shown in Figures 8, 9, 10

and 11 respectively. The pre-launch calibration values, which are fixed and used for operational data processing, are also shown in these figures.

*2) Vicarious calibration results*

Two organizations, the University of Arizona and South Dakota State University (SDSU), have continued to collect ground reflectance and atmospheric measurements concurrent with the Landsat-7 overpasses of their sites [4]. The Arizona measurements are typically at the Railroad Valley and Ivanpah sites (bright, dry lake beds) and the SDSU measurements are at a grass field in Brookings, SD [5].

Four sites have continued to be used for PICS: Sudan 1, Mauritania 1/2, Arabia 1 and Libya 4 per Cosnefroy terminology [9]. The measured responses, converted to radiance, are normalized for variations in illumination conditions of solar zenith angle and Earth-Sun distance [4]. Results for all vicarious methods are presented in figures 8-11. In table 3 the apparent changes in ETM+ gain relative to each calibration source over the life of the mission are presented for all bands.

*3) Discussion*

The lifetime trends in radiometric gain continue to be consistent with those observed over the first 5 years of the mission [4]. The responses to the regularly used calibration lamp 1 are a function of wavelength, being strongest in the blue and smallest in the SWIR bands. The NIR band (figure 9) and the SWIR band 7 actually increased in apparent gain relative to the lamp for a period of time. The responses to the infrequently used lamp 2 showed similar trends, though of smaller magnitude (circa ¼ of lamp 1 values). The changes occurred as a function of lamp usage, not instrument usage, indicating that most of the change was lamp induced. The FASC diffuser trends are a smooth function of wavelength with the peak degradation apparent in the NIR band 4. In band 7, the response to the diffuser increased slightly with

time.  This trend is not consistent with the lamps in magnitude or spectral dependence, again indicating that it is primarily a diffuser change as opposed to an instrument change.

The University of Arizona and South Dakota State University measurements show sufficient scatter that it is difficult to discern any trends in the response.  The PICS sites have less scatter than the traditional vicarious measurements and significantly more data points.  However, seasonal patterns in the PICS site responses complicate the analyses.  Linear fits to the PICS data (table 3) do indicate small (2-3%), but statistically significant, changes in the response in bands 5 and 7.  The systematic seasonal variations limit the statistical validity of the linear fits.  However, these results set an upper bound on the amount of change that may have occurred in these bands that has not been accounted for with the current constant calibration. Attempts are ongoing to beat down the systematic variation in some of the PICS sites.

The PICS site results do not provide absolute calibration information and for purposes of display have been normalized to the pre-launch gains of the instrument.  They thus "match" the pre-launch results, on average, in the plots.  The traditional vicarious measurements  provide absolute calibration information, and the average differences between the vicarious calibration results and the current operational calibration results are presented in table 4.

Key among the observations are:  (1) the operational calibration is within 3% of the Arizona results, which based on the site and the standard deviations of the measurements, is the more precise data set and (2) on average, a bias exists between the vicarious and operational calibration with the vicarious results being lower.

Overall, the ETM+ continues to provide data with absolute calibration uncertainty of 5% or less.  There may be some small-uncompensated trends in one or two bands in the absolute calibration of up to 2% over the 12 years that are difficult to confirm with the techniques available. For most users, this amount of change should not be an issue.  For example, for a target with a surface reflectance of 20%, a 2% relative change translates to less than one half of a reflectance unit delta over the life of the mission. Work is continuing to reduce the uncertainties in PICS methodology with the goal of better quantifying any change.

## IV. CONCLUSION

Landsat-7 ETM+ has been remarkably well behaved and stable radiometrically over its 12 years on-orbit. Although the failure of its scan line corrector has been unfortunate; the remaining Earth-coverage data continue to be valid and valuable.

REFERENCES

[1] NASA. (2011, Mar.). Landsat-7 Science Data Users Handbook. NASA/GSFC, Greenbelt, MD. [Online].

Available: http://landsathandbook.gsfc.nasa.gov/

[2] B. L. Markham, W. C. Boncyk, D. L. Helder and J. L. Barker, " Landsat-7 Enhanced Thematic Mapper

Plus radiometric calibration," *Canadian Journal of Remote Sensing*, vol. 23, pp. 318-332, Dec. 1997.

[3] P. L. Scaramuzza, B. L. Markham, J. A. Barsi and E. Kaita, "Landsat-7 ETM+ on-orbit reflective-band

radiometric characterization," *IEEE Trans. Geosci. Remote Sensing,* vol.42, pp. 2796-2809, Dec. 2004.

[4] B. L. Markham, K. J. Thome, J. A. Barsi, E. Kaita, D. L. Helder, J. L. Barker and P. L. Scaramuzza, "

Landsat-7 ETM+ on-orbit reflective-band radiometric stability and absolute calibration," *IEEE Trans.*

*Geosci. Remote Sensing,* vol.42, pp. 2810-2820, Dec. 2004.

[5] K. J. Thome, D. H. Helder, D. Aaron and J. D. Dewald. "Landsat-5 TM and Landsat-7 ETM+ absolute

radiometric calibration using the reflectance-based method," *IEEE Trans. Geosci. Remote Sensing,*

vol.42, pp. 2777-2785, Dec. 2004.

[6] C. de Vries, T. Danaher, R. Denham, P. Scarth, S. Phinn, and E. H. Miller, "An operational radiometric

calibration procedure for the Landsat sensors based on pseudo-invariant target sites," *Remote Sens.*

*Environ.*, vol. 107, pp. 414-429, April 2007.

[7] G. Chander, X. Xiong, T. Choi, and A. Angal, "Monitoring on-orbit calibration stability of the Terra

MODIS and Landsat 7 ETM+ sensors using pseudo-invariant test sites," *Remote Sens. Environ.*, vol.

114, pp. 925-939, 2010.

[8] B. L. Markham, J. L. Barker, E. Kaita, J. Sieferth and R. Morfitt, "On-orbit performance of the Landsat-

7 ETM+ radiometric calibrators," *Int. J Remote Sens*, vol. 24, pp. 265-285, 2003.

[9] H. Cosnefroy, M. Leroy, and X. Briottet, " selection and characterization of Saharan and Arabian desert

sites for the calibration of optical satellite sensors," *Remote Sens. Environ.*, vol. 58, pp. 101-114, 1996.

TABLE CAPTIONS

Table 1: ETM+ Spectral Bands

Table 2: Detectors with Step Changes in SNR

Table 3. Apparent Changes in Radiometric Gain (percent) based on On-Board and Vicarious Calibrations over first 12 years of Landsat-7 Mission.

Table 4: Differences Between Operational ETM+ Calibration and Vicarious Calibrations: (Vicarious-Operational)/Operational

FIGURE CAPTIONS

Figure 1. ETM+ band 3 SNR at (a) "high" radiance level, 149.6 W/m$^2$ sr µm and (b) "typical" radiance level, 21.7 W/m$^2$ sr µm.

Figure 2.  Power history of coherent noise for representative detectors  (secondary y-axis represents band 5 detector #12 only)

Figure 3.  ETM+ band 5 detector 12 20 kHz noise change in power with instrument time-on.

Figure 4.  Band 5 detector #9 scene average high-gain bias variation since launch.

Figure 5.  Band 5 detector #4 scene average high-gain bias variation since launch.

Figure 6. Band 1 relative gains in low gain mode.

Figure 7. Band 5 relative gains in high gain mode.

Figure 8. Band 3 radiometric gain history based on on-board sources and vicarious calibrations.

Figure 9. Band 4 radiometric gain history based on on-board sources and vicarious calibrations.

Figure 10. Band 5 radiometric gain history based on on-board sources and vicarious calibrations.

Figure 11. Band 7 radiometric gain history based on on-board sources and vicarious calibrations.

**Brian L. Markham** (M'04) received the B.S. degree with a specialization in natural resources in 1976 and the M. S. degree in air photo interpretation/remote sensing in 1978, both from Cornell University.  He received the M.S. degree in applied physics from Johns Hopkins University in 1996.

He has been employed as a physical scientist at NASA's Goddard Space Flight Center since 1978. He has been involved in the radiometric calibration and characterization of the sensors on the Landsat series of satellites, as well as other field, and aircraft instrumentation for 25 + years.  Key activities have included performing and coordinating atmospheric characterization and radiometric calibration of field and aircraft remote sensing instrumentation for the First ISLSCP Field Experiment (FIFE) and the Boreal Ecosystem-Atmospheric Study (BOREAS), leading the radiometric algorithm development team for the Landsat-7 Image Assessment System (IAS), analyzing radiometric characterization results for the Landsat-7 ETM+ and recommending the radiometric calibration updates as necessary, and coordinating the pre- and post-launch radiometric calibration efforts for the Landsat-7 ETM+. Currently he is the Calibration Scientist for Landsat-5, Landsat-7 and the Landsat Data Continuity Mission (LDCM) and the Calibration/Validation Manager for LDCM.


**Md Obaidul Haque** received the B.S. degree in Electrical & Electronic Engineering from Bangladesh University of Engineering & Technology (BUET), Dhaka, Bangladesh in 1996 and the M.S. degree in Electrical Engineering from South Dakota State University (SDSU), Brookings, SD in 2005.

He is currently with Stinger Ghaffarian Technologies, Inc., Greenbelt, MD, a contractor to the U.S. Geological Survey Earth Resources Observation and Science Center, Sioux Falls, SD. He is a Radiometric Calibration Engineer working on the Landsat Image Assessment System to monitor and analyze radiometric trending for sensor characterization and calibration. He also contributed on the development of the Landsat 5 Thematic Mapper Image Assessment System.

**Julia A. Barsi** received the B.S. and M.S. degrees in imaging science with a concentration in remote sensing from the Rochester Institute of Technology, Rochester NY. She is currently a calibration analyst with Science Systems and Applications, Incorporated, Greenbelt MD. She is involved with the characterization and calibration of the Landsat sensors, with an emphasis on the thermal band calibration.

**Esad Micijevic** received the B.S. degree in electrical engineering from the University of Zagreb, Zagreb, Croatia, and the M.S. degree in engineering from South Dakota State University, Brookings.

He has been working on Landsat radiometric and geometric characterization and calibration since 2001. He is currently a Calibration Engineer with Stinger Ghaffarian Technologies, Inc., Greenbelt, MD, a contractor to the U.S. Geological Survey Earth Resources Observation and Science Center, Sioux Falls, SD. His primary focus is on the development of radiometric calibration and characterization algorithms and processing system for the Landsat Data Continuity Mission, the analysis of Landsat radiometric data trends and the development and generation of Landsat calibration parameter files.

**Dennis L. Helder** received the B.S. and M.S. degrees in electrical engineering from South Dakota State University and the Ph.D. in engineering from North Dakota State University.

He has been involved with radiometric calibration of the Landsat series of instruments since 1988. He founded the SDSU Image Processing Laboratory in 1991 and is the current director. He has been involved with the Landsat 7 Science Team, the EO-1 Science Validation Team, and is currently a member of the Landsat Data Continuity Mission Science Team. Helder is currently the Associate Dean for Research in the College of Engineering at South Dakota State University

**Kurtis J. Thome** obtained a BS degree in Meteorology from Texas A&M University and MS and PhD degrees in Atmospheric Sciences from the University of Arizona.

He then joined what is now the College of Optical Sciences becoming full professor in 2006. He served as the Director of the Remote Sensing Group from 1997 to 2008. Thome moved to NASA's Goddard Space Flight Center in 2008 as a Physical Scientist in the Biospheric Sciences Branch. He has been a member of the Landsat-7, ASTER, MODIS, and EO-1 Science Teams providing vicarious calibration results for those and other imaging sensors. He is a Fellow of SPIE and is serving as the calibration lead for the Thermal Infrared Sensor on the Landsat Data Continuity Mission and is the Deputy Project Scientist for CLARREO for which he is also the instrument lead for the Reflected Solar Instrument.

**David Aaron** is an Assistant Professor of Physics at South Dakota State University. He received his B.S. in Engineering Physics at SDSU, an M.S. in Materials Science at the University of Wisconsin-Madison, and worked in the Aerospace industry in design and assessment of high power laser diodes.
He has been working on radiometry and vicarious calibration of satellite sensor systems since 2002. Recent primary studies have included using pseudo-invariant sites to back-calibrate Landsat MSS sensors, with these results being incorporated in the USGS processing algorithms to provide a consistent calibration of the entire Landsat sensor series. Enhancements to the techniques used are presently being studied to further improve the understanding of past, present, and future on-orbit calibration of Landsat and other space-born sensors.

**Jeff Czapla-Myers** is an Assistant Research Professor in the College of Optical Sciences at the University of Arizona. He obtained the B.S. degree in Optical Engineering from the University of Arizona in 1997, the M.Sc. degree in Earth and Space Science from York University (Toronto, Canada) in 2000, and the Ph.D. degree in Optical Sciences from the University of Arizona in 2006. His research interests include remote sensing, radiometry, ground-based vicarious calibration of airborne and satellite systems, and the design, development, and laboratory characterization of radiometers.

Brian L. Markham



Md. Obaidul Haque



Julia A. Barsi

Esad Micijevic



Kurtis J. Thome

Table 1

| Band | Bandpass (nm) | IFOV (m) | Detectors |
|---|---|---|---|
| 1 | 441-514 | 30 | 16 |
| 2 | 519-601 | 30 | 16 |
| 3 | 631-692 | 30 | 16 |
| 4 | 772-898 | 30 | 16 |
| 5 | 1547-1748 | 30 | 16 |
| 6* | 10.31-12.36 μm | 60 | 8 |
| 7 | 2065-2346 | 30 | 16 |
| 8 (Pan) | 515-896 | 15 | 32 |

* Not discussed in this paper

Table 2

| Band | Detector | Date of change | Low Signal Change (%) | High Signal Change (%) |
|------|----------|----------------|-----------------------|------------------------|
| 2 | 6 | Apr 2008 | 1.8 | 1.0 |
| 2 | 8 | Sep 2008 | 1.7 | 1.0 |
| 3 | 6 | Sep 2008 | 2.3 | 1.5 |
| 8 | 6 | May 2009 | 1.4 | 1.1 |
| 8 | 18 | Oct 2010 | 2.2 | 1.6 |
| 8 | 25 | Apr 2009 | 2.0 | 1.5 |
| 8 | 26 | Jan 2010 | 1.6 | 1.2 |

Table 3

| Band | Lamp 1 | Lamp 2 | FASC | PICS (linear fit) | |
|---|---|---|---|---|---|
| | | | | Change | Uncertainty |
| 1 | -28.3 | -6.8 | -7.1 | -1.1 | 0.4 |
| 2 | -24.8 | -4.6 | -7.0 | -0.3 | 0.2 |
| 3 | -19.5 | -4.0 | -8.5 | -0.2 | 0.2 |
| 4 | -3.8 | +0.8 | -11.8 | -1.3 | 0.4 |
| 5 | -7.2 | -0.8 | -2.4 | -2.2 | 0.3 |
| 7 | -1.9 | -0.9 | 1.9 | -2.7 | 0.5 |
| Pan | -10.0 | -2.5 | -9.0 | -0.4 | 0.4 |

Table 4

| Band | University of Arizona (n~95) | | South Dakota State University (n=31) | |
|------|----------------------------|----------------------------|----------------------------|----------------------------|
| | Mean Difference (%) | Standard Deviation (%) | Mean Difference (%) | Standard Deviation (%) |
| 1 | -3.3% | 2.4% | 1.2% | 4.9% |
| 2 | -2.7% | 3.3% | -0.2% | 6.1% |
| 3 | 0.6% | 3.1% | -0.6% | 7.0% |
| 4 | -0.6% | 2.8% | -1.1% | 5.2% |
| 5 | -2.9% | 2.4% | -7.2% | 5.6% |
| 7 | -2.2% | 2.9% | -7.6% | 6.9% |
| Pan | - | - | - | - |
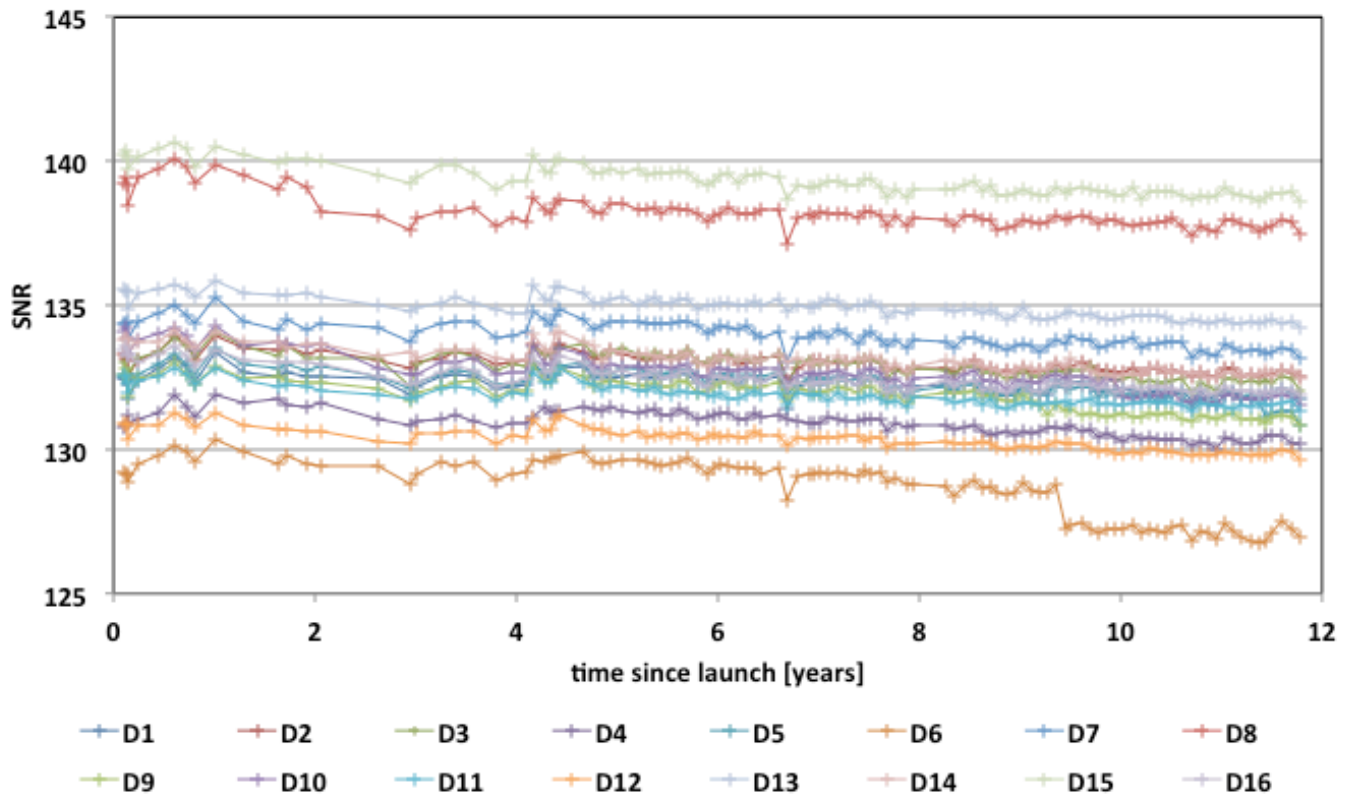
Figure 1a
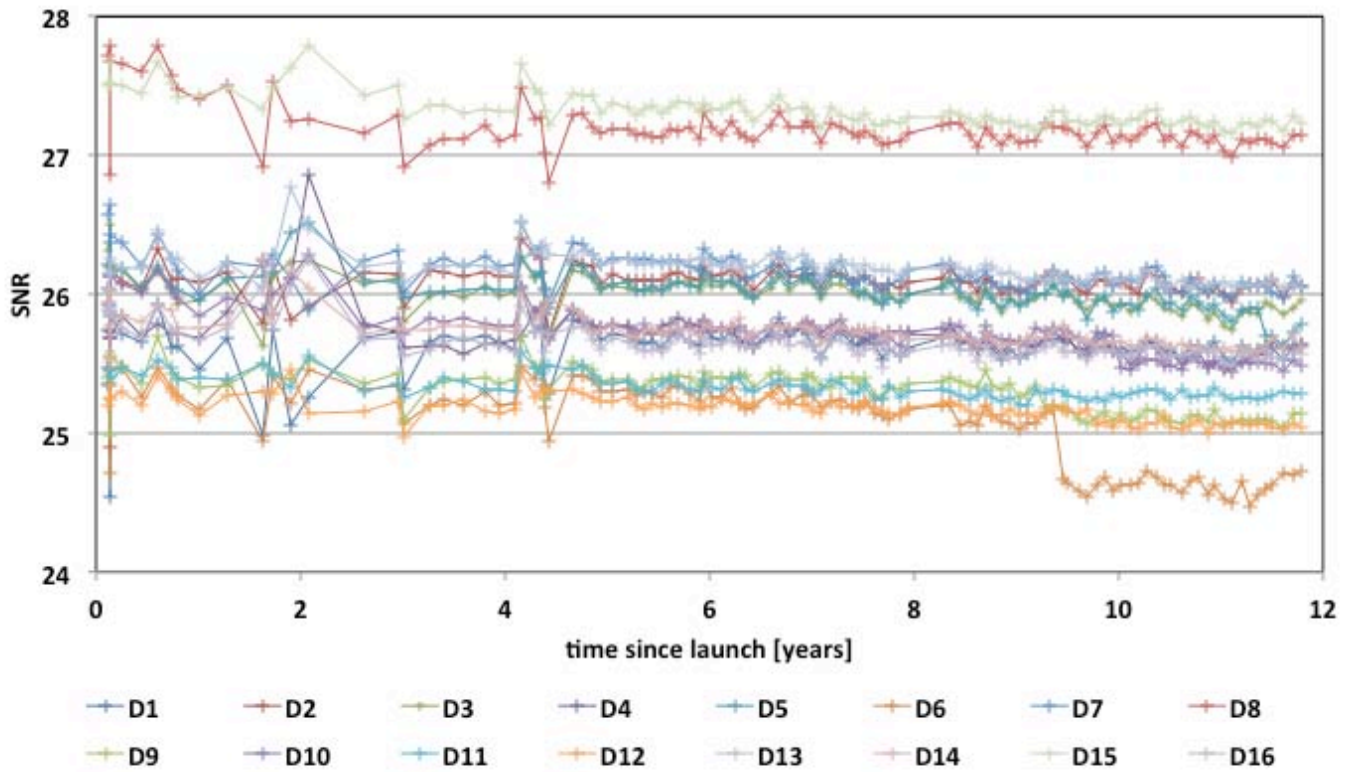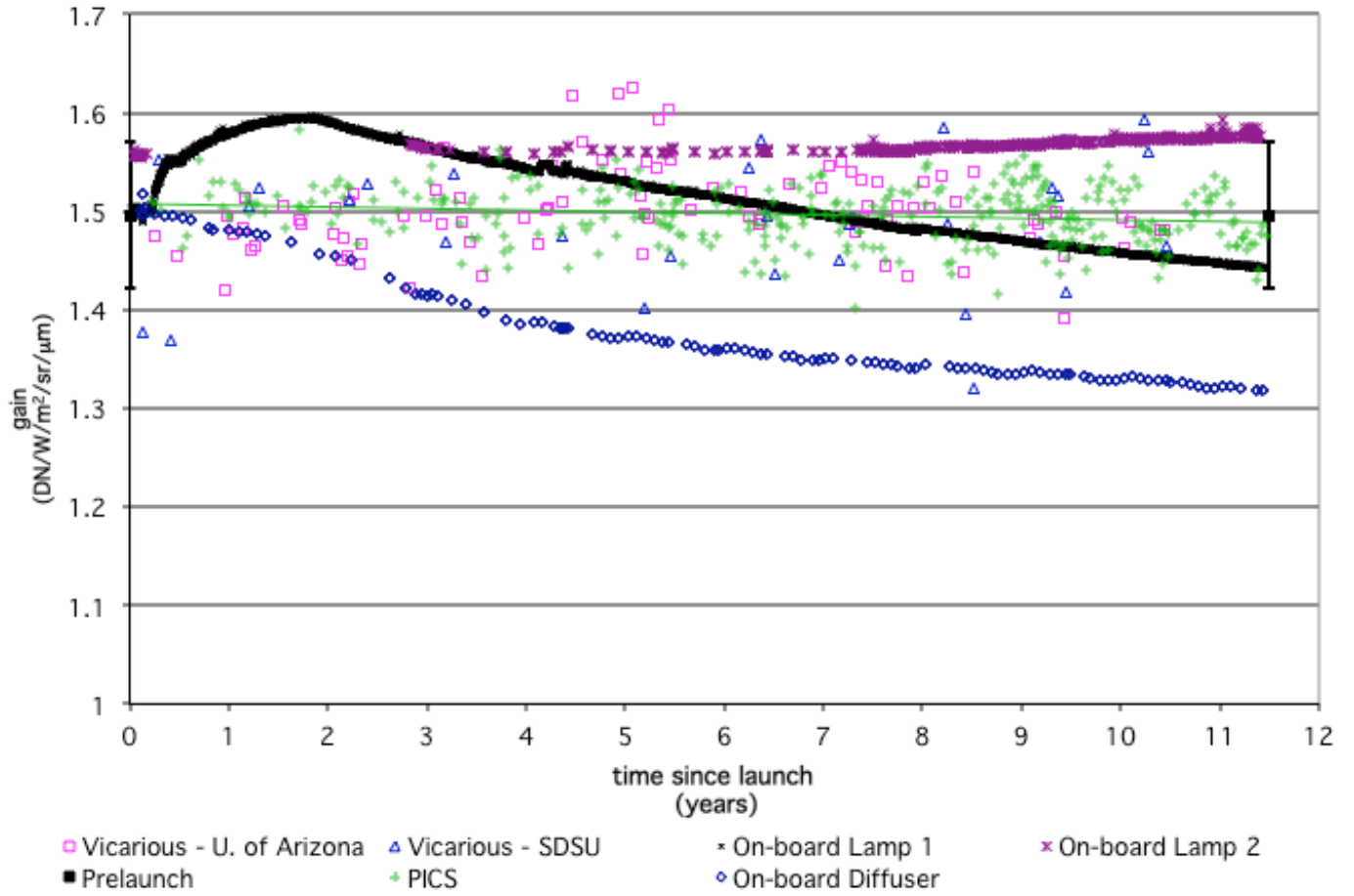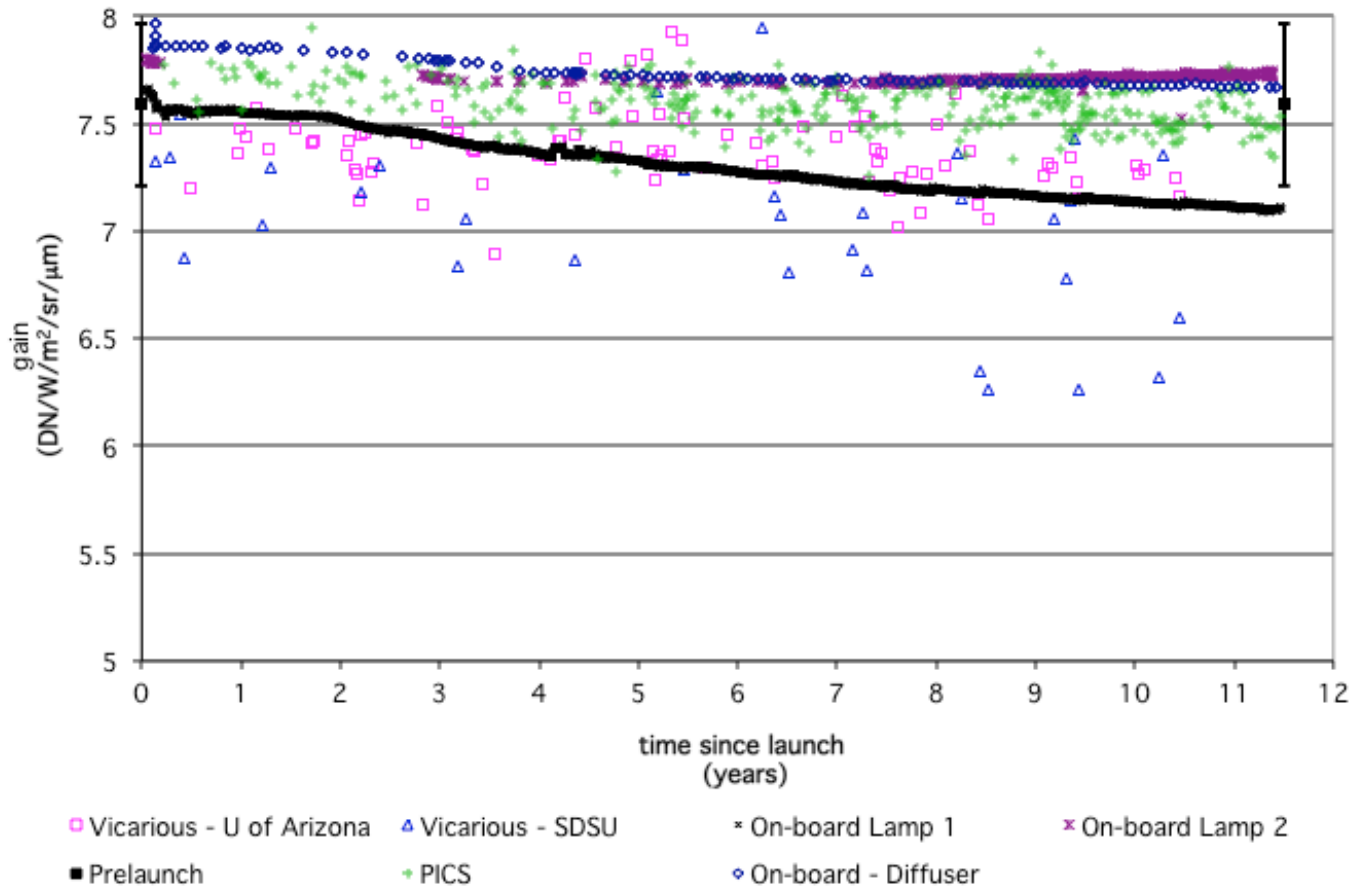


Figure 1b
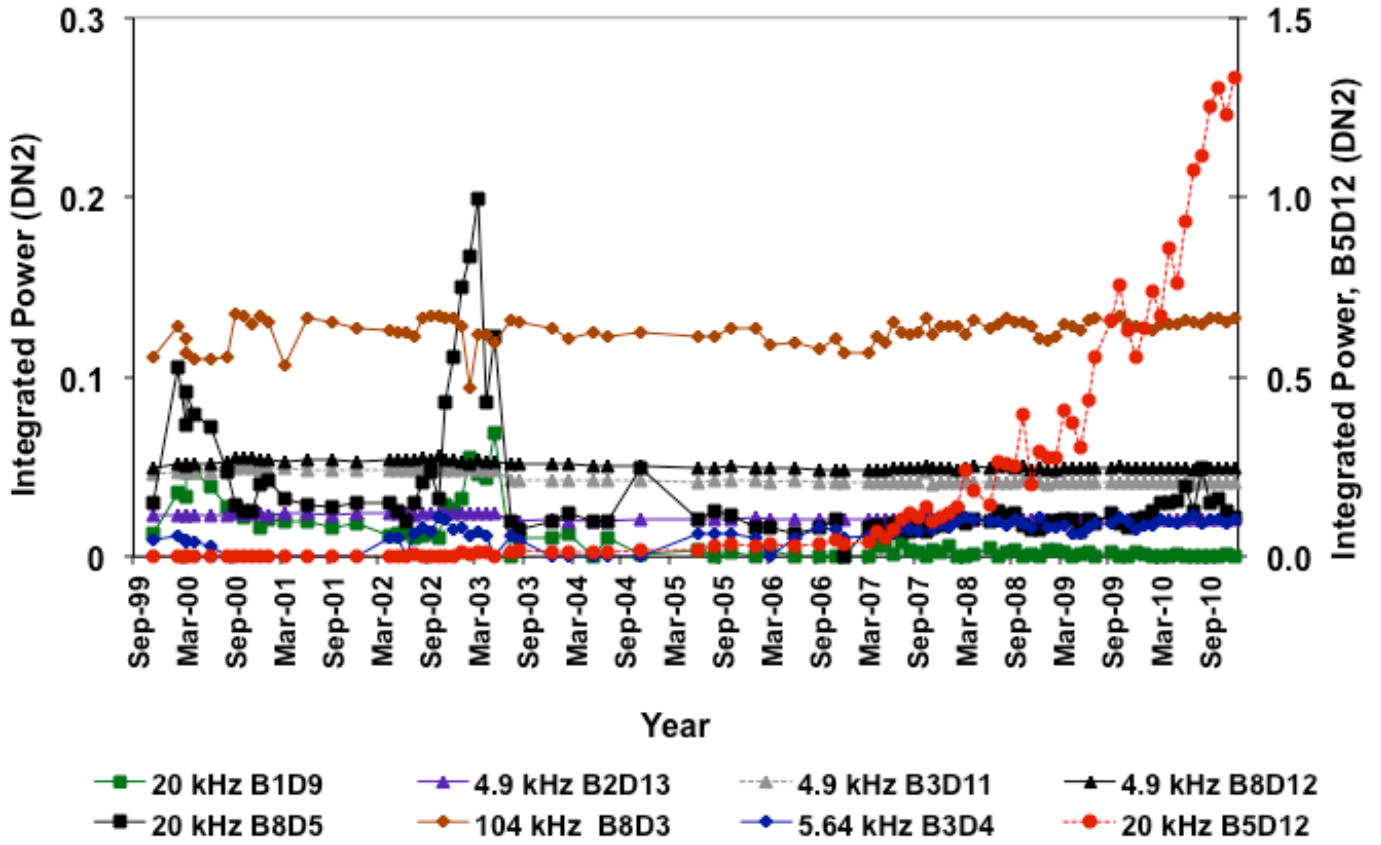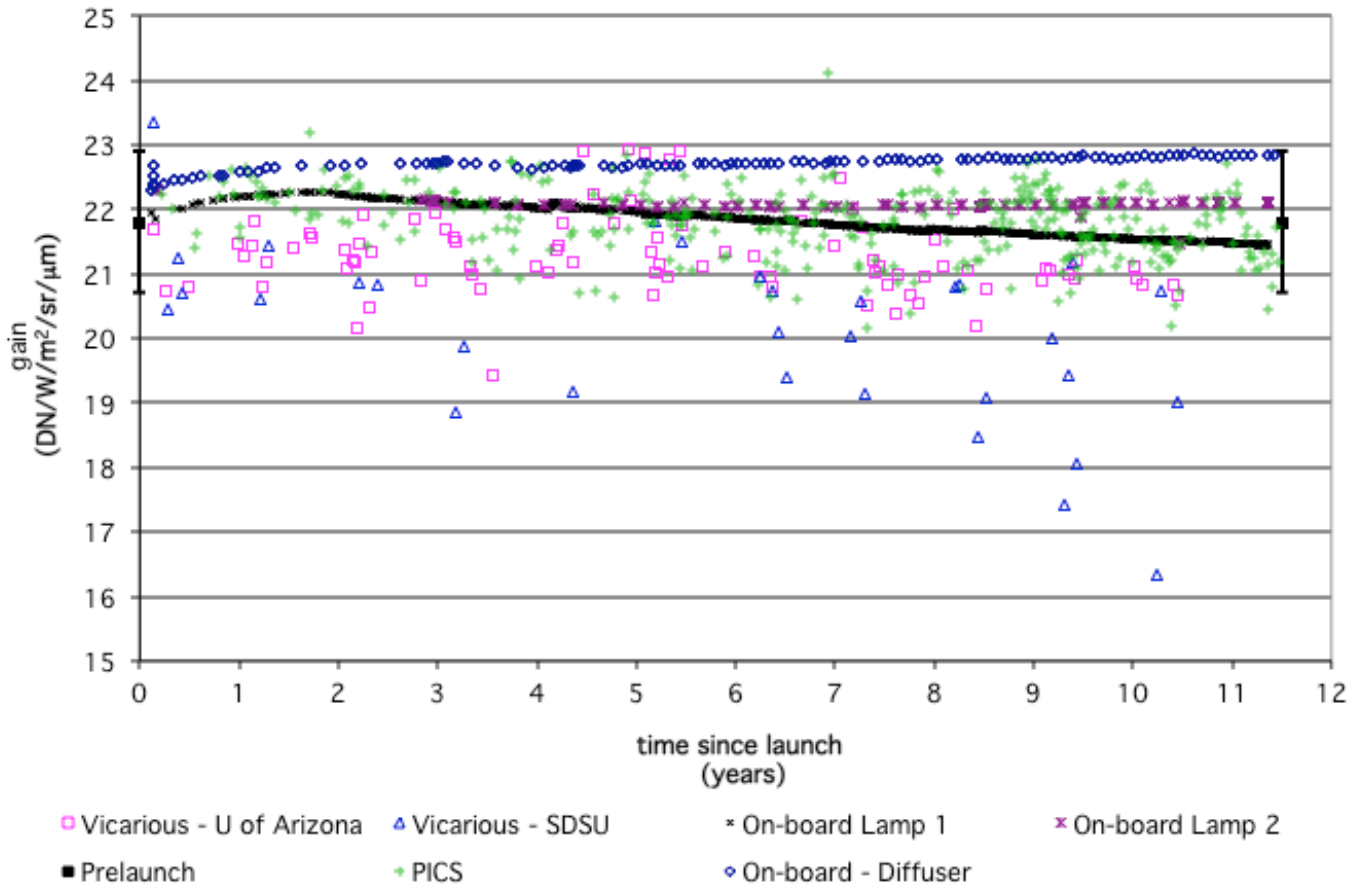
Figure 2
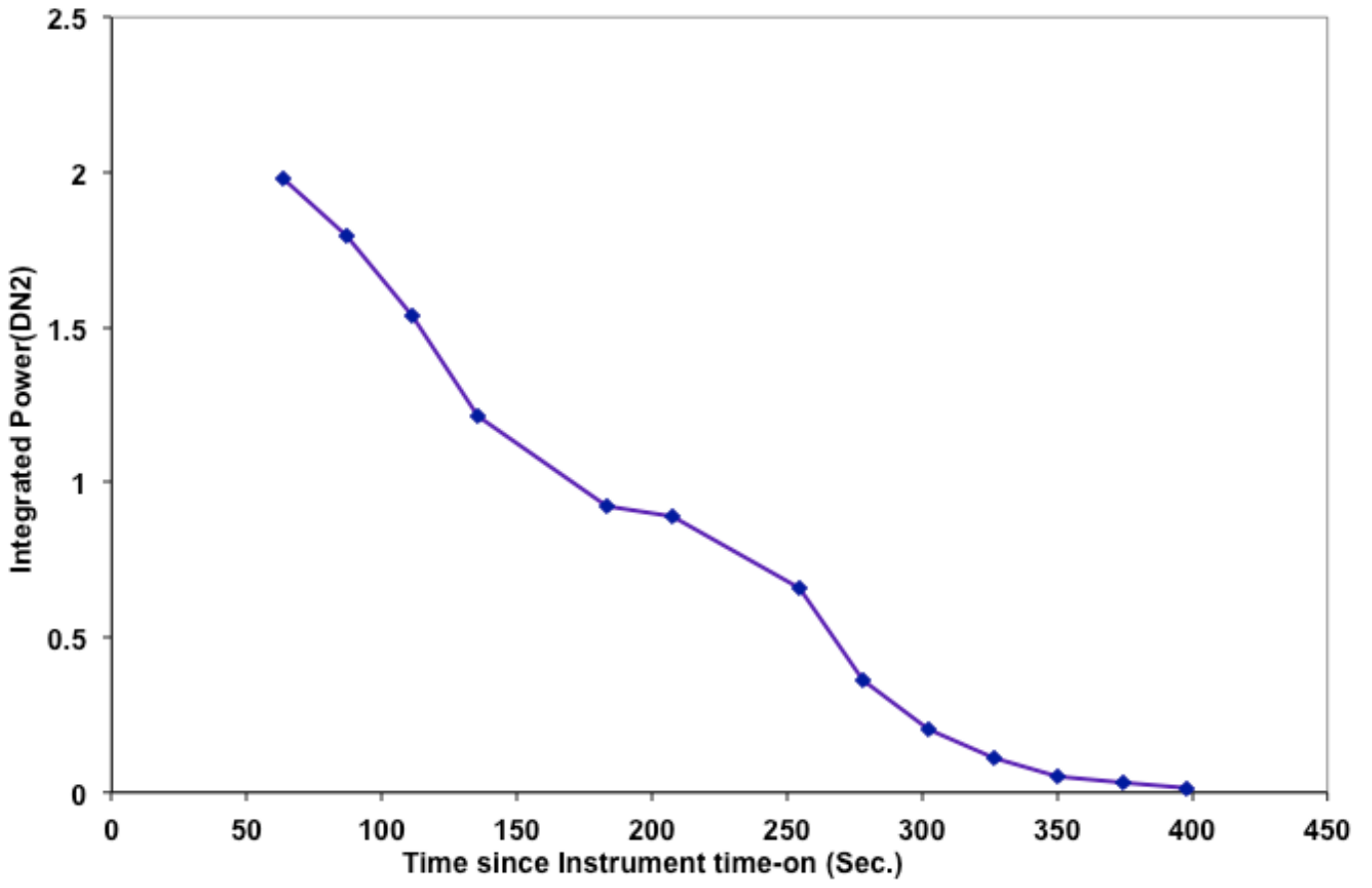
Figure 3
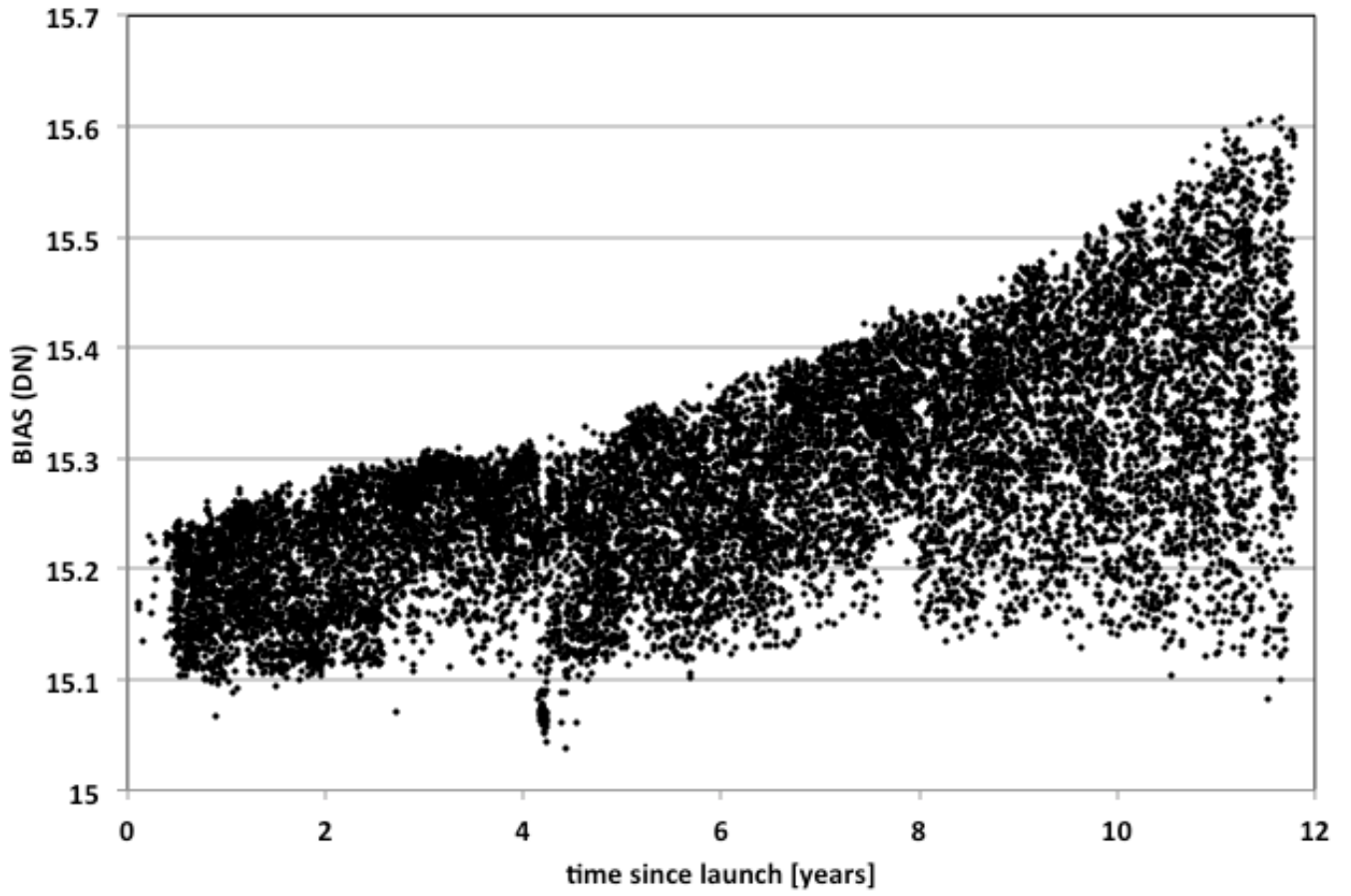
Figure 4
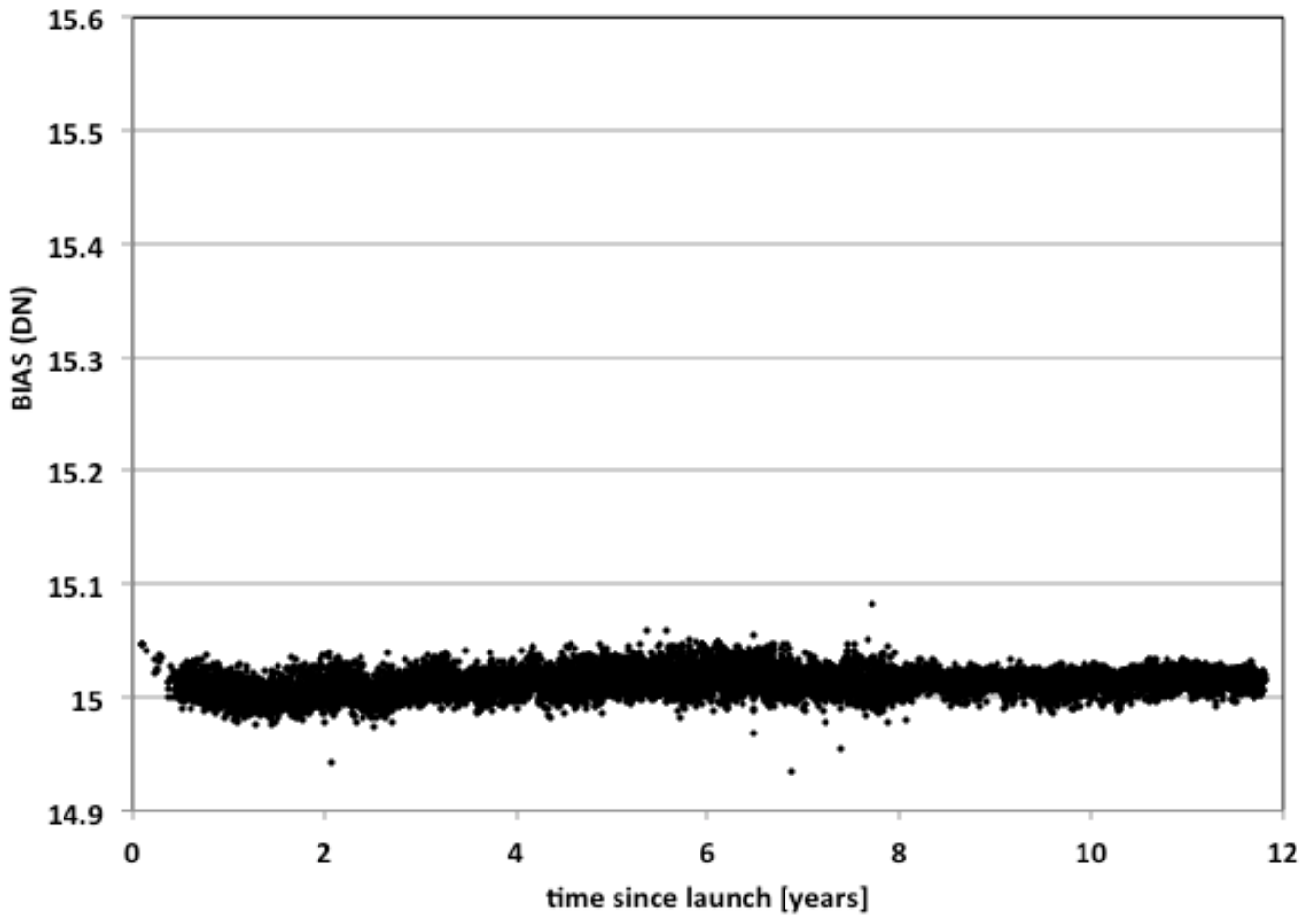
Figure 5
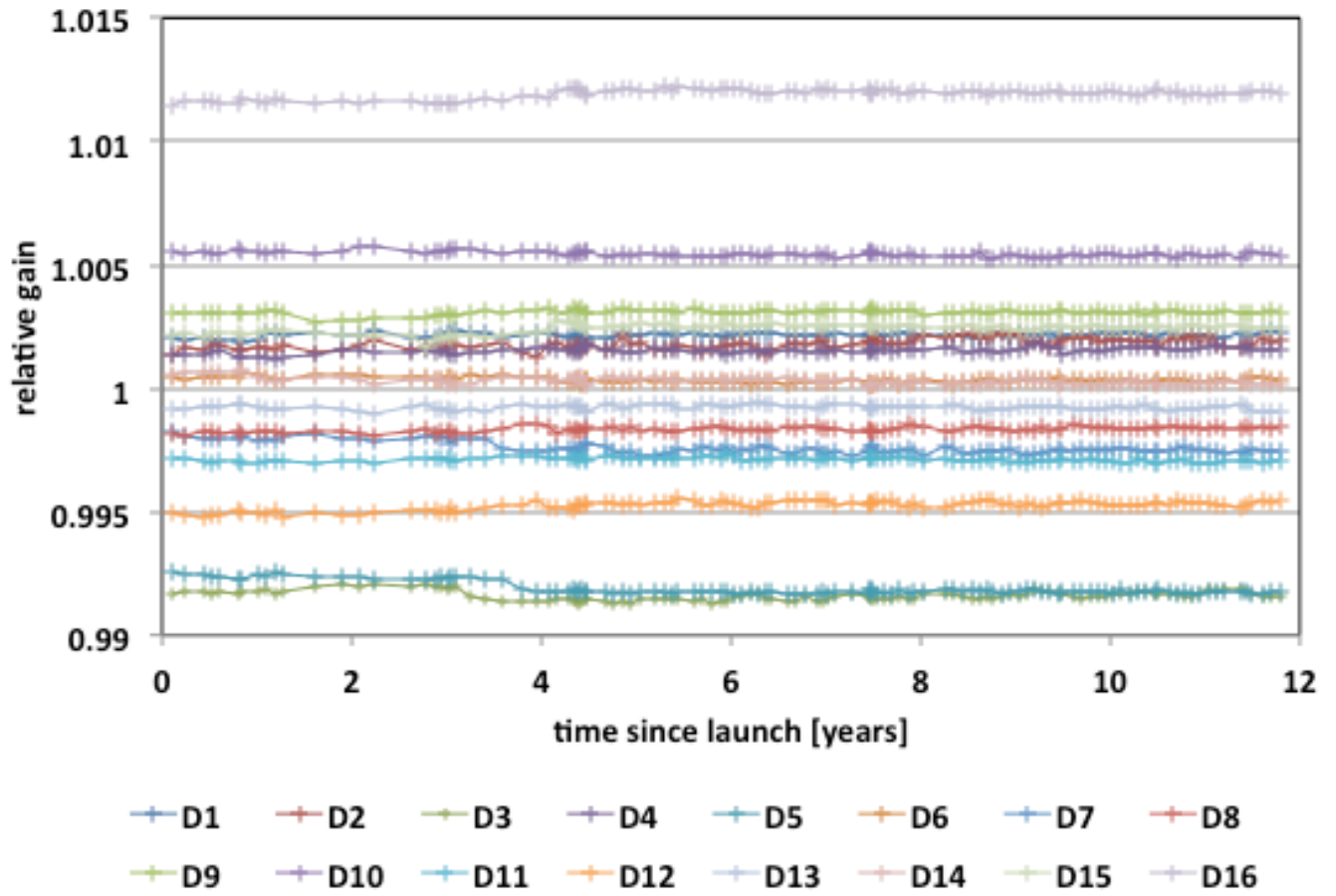
Figure 6
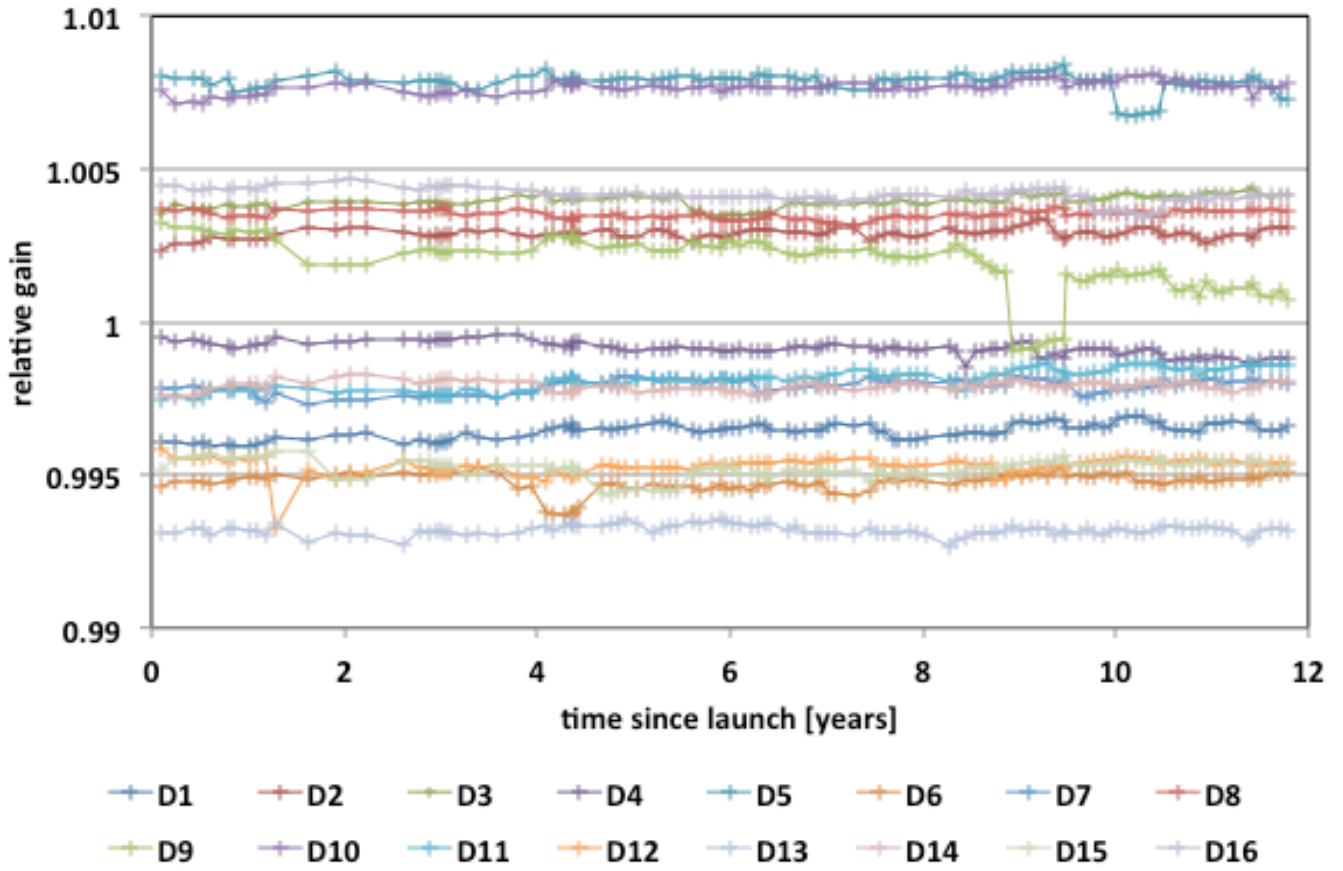
Figure 7
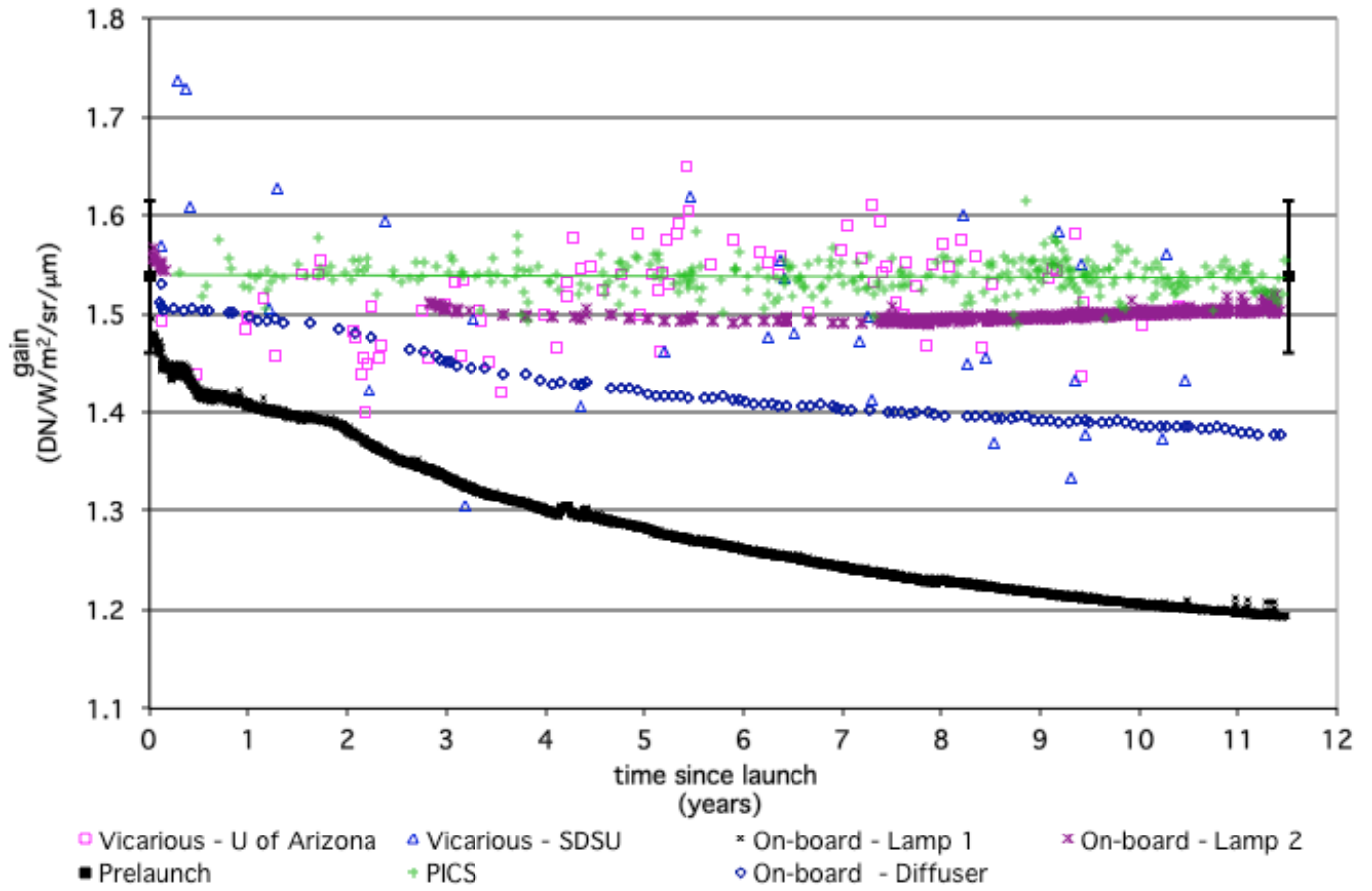
Figure 8

Figure 9

Figure 10

Figure 11